PERGAMON

Deep-Sea Research I 49 (2002) 1291–1305

DEEP-SEA RESEARCH
PART I

www.elsevier.com/locate/dsr

Instruments and Methods

In situ ultraviolet spectrophotometry for high resolution and long-term monitoring of nitrate, bromide and bisulfide in the ocean

Kenneth S. Johnson*, Luke J. Coletti

Monterey Bay Aquarium Research Institute, 7700 Sandholdt Road, Moss Landing, CA 95039, USA

Received 19 October 2001; received in revised form 19 March 2002; accepted 21 March 2002

Abstract

The design for an in situ ultraviolet spectrophotometer (ISUS) that can operate while submerged to depths of at least 2000 m is reported. We show that the ISUS can be used to make high resolution ($\sim$1/s and 0.5 cm) and long-term (>3 months) measurements of the concentration of nitrate, bisulfide and bromide in seawater using the distinctive, ultraviolet absorption spectra of these chemical species. The precision, accuracy and stability of the chemical concentrations derived with the ISUS are sufficient for many biogeochemical studies. One standard deviation of the nitrate concentration in seawater is $\sim$0.5 μM and the limit of detection (3 SD) for one observation would be $\sim$1.5 μM. However, the noise is nearly random and significant reductions in the detection limit are possible by averaging multiple observations. The 95% confidence interval for a 30 s scan is 0.2 μM. Low temperatures appear to produce a bias ($\sim$10% at 400 m depth in the ocean) in the nitrate concentration and in the salinity estimated from the bromide concentration. If an independent estimate of salinity is available, then the bias in nitrate can be eliminated by correcting nitrate concentrations by the same amount that the optical estimate of salinity is in error. The instrument has been deployed on a mooring in the equatorial Pacific for a 6-month period with no apparent degradation in performance during the first 3 months. Measurements of UV spectra at a height of 1 cm over the bottom in a cold seep at 960 m depth demonstrate the capability to detect bisulfide ion within the benthic boundary layer.

Keywords: Nitrates; Hydrogen sulfide; Sea water; Water analysis; Analytical techniques

1. Introduction

There has been an extensive effort to design chemical sensors and analyzers that are capable of operating in situ. Much of this work has been summarized in two recent volumes on chemical sensor systems for aquatic sciences (Varney, 2000; Buffle and Horvai, 2000). These volumes describe a variety of continuous flow analyzers, electrochemical sensors and optical sensors for in situ measurements of dissolved chemical species. However, there are no instruments that are capable of high resolution (response rate $\leqslant$ 1 s), high precision (<0.5 μM), high accuracy (<1%) and long-term

*Corresponding author. Tel.: +1-831-775-1985; fax: +1-831-775-1620.

E-mail address: johnson@mbari.org (K.S. Johnson).

0967-0637/02/$ - see front matter
PII: S0967-0637(02)00020-1

(> 1 yr) measurements of dissolved nitrate or hydrogen sulfide. Such performance is required to sample large areas of the ocean or complex regions near deep-sea hydrothermal vents (Johnson et al., 1986). The lack of real-time, in situ monitoring of dissolved chemical species may lead to chronic undersampling of episodic processes (Dickey et al., 1991; Johnson and Jannasch, 1994; McGillicuddy et al., 1998). Such instruments will be critical to the development of ocean observatories (National Research Council, 2000).

Many dissolved inorganic compounds absorb light at wavelengths <280 nm in the ultraviolet (e.g. Buck et al, 1954; Collos et al., 1999). Among these are compounds of interest to aquatic scientists, including nitrate, nitrite, bisulfide (HS^-) and bromide (Fig. 1). Ogura and Hanya (1966) examined the UV spectra of seawater and found that the signal was dominated by bromide, nitrate and, to a much lesser extent, organic matter. Several other inorganic ions, including carbonate, have weak UV absorption spectra. Their concentrations in seawater are too low for direct detection.

Several analytical methods have been developed in the past 40 yr for the direct determination of nitrate based on measurement of its UV absorption with laboratory spectrophotometers (e.g., Bastin et al., 1957). These techniques include an American Public Health Association standard method for nitrate analysis (Clesceri et al., 1989). Armstrong and Boalch (1961) briefly considered the determination of nitrate in seawater by direct UV spectroscopy. More recently, Collos et al. (1999) have shown that direct UV spectroscopy could be used for nitrate measurements in plankton cultures. An instrument for in situ determination of nitrate by measurement of UV absorption at six wavelengths has also been developed (Finch et al., 1998; Clayson, 2000). The results obtained with this instrument clearly show the potential to make in situ measurements of nitrate concentration by measuring UV absorption signals.

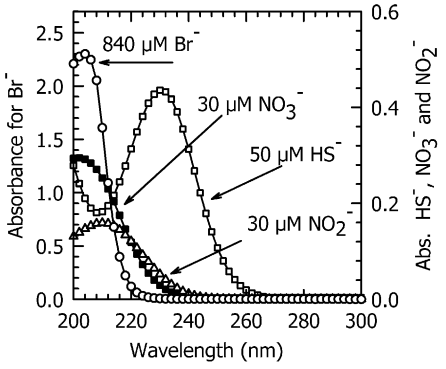

Fig. 1. Absorption spectra of bromide, bisulfide, nitrate and nitrite at concentrations typical of seawater. Each salt was dissolved in deionized water. Spectra were collected with a Hewlett-Packard HP 8452 spectrophotometer. Cell path length was 1 cm. Note that the left axis applies to bromide and the right axis to the other species.

These laboratory and in situ methods for nitrate determination have not become widely used, in part, because most of the analytical methods were based on measurements at one or a few wavelengths. Measurements at a small number of wavelengths do not allow robust techniques to be used for separation of overlapping spectra. Spectral deconvolution techniques (Rutan, 1991; Berger et al., 1998; Thomas and Gallot, 1990) make it feasible to determine these compounds directly in complex media, such as seawater, without significant interferences, and with no chemical manipulations. Robust, multiwavelength methods for nitrate determination have already been used in such difficult solutions as unfiltered, waste water and ground waters (Thomas et al., 1990; Karlsson et al., 1995; Holm et al., 1997). Menzel et al. (1997) examined the potential of several multivariate calibration methods for UV determination of nitrate in seawater and they concluded that classical least-squares methods were most satisfactory.

We have confirmed, by using a bench top Hewlett-Packard HP8452 spectrophotometer operated on an oceanographic cruise during March 1998 off Central California that nitrate and bromide concentrations in coastal seawater can be accurately (<3%) determined by measurement of the UV spectrum. The relationship between UV-based estimates of nitrate concentration (NO_3UV) and concentration determined with an Alpkem RFA segmented flow analyzer (NO_3RFA;

Sakamoto et al., 1990) was $NO_3UV = -0.14 + 0.981 \times NO_3RFA$ ($n = 183$, $R^2 = 0.997$) for concentrations from 0 to 44 μM. We have also demonstrated in the laboratory that total sulfide ($H_2S + HS^- + S^{2-}$ + reactive polysulfides) could be determined in a variety of natural samples, including sediment pore waters and hydrothermal fluids, by deconvolving the UV absorption spectrum (Guenther et al., 2001). Further, advances in the development of diode array spectrophotometers (Smith, 2000) and low power UV light sources (Huebner et al., 2000) now make it possible to rapidly collect full spectra in the UV region using compact instruments that are amenable to operation in situ.

Here, we report the development of an in situ ultraviolet spectrophotometer (ISUS) system with high spectral resolution (<1 nm) that can operate throughout the ocean and, presumably, in fresh waters, on conductivity temperature depth (CTD) profilers, undulating towed vehicles, remotely operated vehicles or on deep-sea moorings. The high spectral resolution allows us to deconvolve the spectra of nitrate, bromide and bisulfide in natural samples. We demonstrate that measurements of nitrate, bromide and bisulfide can be made in situ at the accuracy and precision required for many oceanographic studies. Response time is on the order of 1 s and the instrument is capable of operating >1 yr at five samples per day. Such measurements are quite simple, as no chemical manipulations are required. This makes direct optical determination of UV-absorbing compounds a relatively simple and robust analysis.

2. Methods

2.1. Instrument design

The instrument is composed of four key components: the UV light source, an optically coupled sensing probe, the high resolution spectrometer and a low power instrument controller with large amounts of data storage (Fig. 2). Keys to successful detection of nitrate, bromide or sulfide, in an environment where many other compounds may absorb in the UV region, are a stable, high resolution (~1 nm) spectrometer with good sensitivity in the UV region and a stable light source. We selected a Zeiss MMS series, photodiode array (PDA) spectrometer optimized for the ultraviolet (Zeiss MMS UV) with a spectral range of 200–400 nm. Photodiode array detectors generally have a superior sensitivity and stability in the UV region when compared to other solid state detectors. The 256 element MMS UV spectrometer provides high resolution (0.8 nm) in the spectral range of interest without having an excessive number of detector elements (pixels) to read out. The spectrometer was fitted with signal processing electronics manufactured by Spectronic Devices, Ltd. (CRO-MMS UV). The CRO-MMS UV digitizes each element of the array with a 16-bit analog to digital converter. Commands for digitizing the spectrometer's 256 element PDA and transferring the data are made through a bi-directional parallel interface conforming to the IEEE-1284 enhanced parallel port (EPP) specification.

We tested a pulsed xenon light source (EG&G RSL2100) and a continuous wave deuterium light

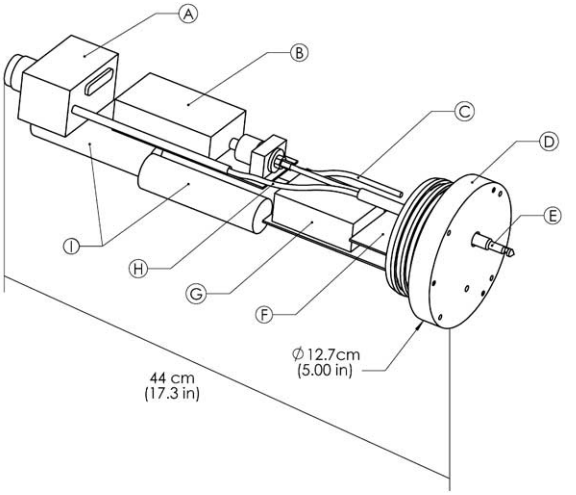

Fig. 2. Block diagram of ISUS components: (A)—spectrometer, (B)—UV light source, (C)—UV fiber to reference detector, (D)—pressure housing end cap, (E)—retroreflection probe, (F) –reference channel board, (G)—Model 8 controller, Compact Flash RAM and motherboard, and (H)—UV fiber from retroreflection probe to spectrometer. Three lithium DD size batteries (I) fit under the UV light source in the 10.2 cm inside diameter pressure housing.

source (Hereaus Fiberlight). Three problems arose with the xenon flash sources. The light intensity of the xenon flash was relatively low in the spectral region (<220 nm) where nitrate absorption is high and there were large changes in intensity (>20×) from 210 to 300 nm. Long integration times could not be used to increase signal at low wavelengths because the high signal at greater wavelengths saturated the detector array. The large variability in the xenon lamp spectra was also problematic under conditions of larger temperature variability. Finally, the relatively high intensity of the xenon source caused solarization of optical fibers, which changed their optical properties. Solarization resistant, quartz fibers (Huebner et al., 2000) were used to minimize this problem. However, solarization still remained a problem with the xenon flash lamps.

A Hereaus Fiberlight, which is a low power (3 W), line free, continuous wave deuterium light source that employs a high frequency alternating current for excitation, was tested as an alternative. The Fiberlight was found to have good stability, greater relative output in the spectral region where nitrate absorbs, relatively low variation in intensity (2.5×) from 210 to 300 nm, and it did not produce detectable solarization in the fibers. The Fiberlight also requires little warm up time, which allows the instrument to be turned on and a complete spectrum collected in a few seconds. All subsequent work reported here was performed using Fiberlight sources.

Light was passed through seawater using fiber-optically coupled retroreflection probes from either Equitech International or C-Technology. A 600 μm fiber from the light source was connected to the retroreflection probe input. A single fused Si lens images UV light from the lamp fiber into a fixed volume of sample solution. The UV light passes through the solution into a fused Si window and onto a sealed UV mirror. Reflected light returns through the same optical path and is imaged onto the output fiber. The retroreflection probe output was connected to the Zeiss spectrometer with a single 600 μm quartz fiber. The effective path length is double the illuminated length of the probe.

The Equitech probe body is made of polyether etherketone (PEEK) and rated to 200 bar pressure and 280°C, while the C-Technology probe body is constructed from stainless steel with no specified pressure or temperature rating. We have utilized the C-Technology probe to depths of 1000 m (~100 bar). The distal ends of both probes, which hold the second lens and mirrored reflection surface, are screwed onto the probe bodies. This allows the cell path length to be easily changed. All of the work described here was conducted with a 1 cm light path (0.5 cm illuminated length), except for the HS^- measurements, which used a 0.5 cm light path.

A second fiber from the UV light source was routed to a SiC UV sensitive reference diode (Boston Electronics JEC01S). The SiC photodiode has a sensitivity from 210 to 380 nm (10% of maximum response) with a peak response at 270 nm. The output of the SiC photodiode can be used to provide a reference channel to monitor light output from the Fiberlight. However, none of the results discussed here were corrected for intensity variations. Changes in light intensity were found to be nearly proportional across the spectral region that we utilize for signal deconvolution, which causes only a constant or, at worst, linear change in intensity. The light intensity change is subsumed in the baseline terms of the spectral model discussed below and the reference channel was not required to correct spectra for intensity changes. The reference channel was only used to verify that the UV lamp was operating and, in several long-term deployments, to confirm that decreases in intensity monitored with the spectrometer were due to fouling of the retroreflection probe, rather than a reduction in light output.

The ISUS is controlled by an Onset Computer Co. TattleTale Model 8 data logger, which is based on a 16 bit Motorola 68332 microprocessor. Data storage on the Model 8 logger was augmented using a Persistor Inc. Model CF8 Compact Flash (CF) memory adapter, which can support CF memory cards up to 300 MB. This permitted complete spectra to be stored during extended deployments, as well as the calculated chemical concentrations. Three custom-printed circuit boards were designed to integrate the system components. A CPU motherboard connects to

the Model 8's digital input/output lines and interfaces the data logger with system components. An EPP bi-directional parallel interface for communications with the spectrometer electronics was implemented using a digital port on the Model 8 and support circuitry on the CPU motherboard. A reference channel board held the SiC UV photodiode and amplification circuitry. The 12-bit analog to digital converter that is incorporated in the Model 8 was used to digitize this signal. The reference channel signal was digitized 100 times during each sample reading to maximize the signal to noise ratio.

A power supply board was used to regulate input power from various supplies, including 10 V Li battery packs for autonomous operation or 7–24 V direct current supplies from remotely operated vehicles. This power supply board provided +5 V for the Model 8 and the spectrometer system and +12 V for the Fiberlight. The ISUS requires 3.5 W for continuous operation.

All of the embedded application software used to control the ISUS and to process data onboard the Model 8 was written in ANSI C (Aztec C68k version 5.2D) and native 68000 assembly code. Software to reprocess the ISUS data and to observe the instrumental operation in real time was written in Microsoft Visual Basic.

2.2. Data processing

The wavelength at each pixel on the detector array was determined from a calibration polynomial supplied by Zeiss with each spectrometer. The absorbance at each pixel was calculated from the formula:

$$A_\lambda = -\log((I_\lambda - I_D)/(I_{\lambda,0} - I_D)), \quad (1)$$

where I_λ is the detector intensity (counts) at wavelength λ for light passing through a sample, $I_{\lambda,0}$ is the detector intensity (counts) at wavelength λ for light passing though deionized water and I_D is the detector dark current. The dark current is constant, within detector noise, across the photodiode array. A single value of I_D was used to estimate dark current across the array on a given spectral scan. The dark current does increase significantly with temperature and with detector integration time, however. Each scan may, therefore, require a different estimate of dark current. Several methods were used to estimate the dark current for each scan. The Hereaus Fiberlight has a shutter that could be periodically closed to estimate dark current. Estimates determined by this method were used until the shutter was closed again and a new dark current value was estimated. Intervals between dark current estimates were typically on the order of 10–20 min. Useful concentration data are not collected during the periods when dark current is estimated by this method and the dark current may change due to temperature during the period between estimates. A second method of estimating dark current makes use of the fact that, in seawater, the absorptivity is sufficiently high at wavelengths below 207 nm that undetectable amounts of light are transmitted to the detector array in this region. The dark current could, therefore, be estimated using the mean detector intensity measured at wavelengths <207 nm on each scan. This eliminated the need to periodically close the shutter and it eliminated errors due to changes in the dark current during periods shortly after the instrument was turned on and it was rapidly warming up. Also, the shutter malfunctioned on one occasion during rough sea conditions when the ISUS was being deployed on a mooring. Using the lowest wavelengths to estimate dark current has since allowed us to remove the shutter and eliminate a potential failure mode.

Chemical concentrations can be determined using the Beer–Lambert law:

$$A_\lambda = b(\Sigma_J \varepsilon_{\lambda,J} C_J), \quad (2)$$

where b is the path length (cm) of the optical cell, $\varepsilon_{\lambda,J}$ is the molar absorptivity of chemical species J (l/mol/cm) at wavelength λ, C_J is the concentration (mol/l) of the Jth chemical species that absorbs, and the sum runs over all chemical species J that absorb light in the ultraviolet region. The spectra of the inorganic species in seawater are well defined and the array of molar absorptivities for each species can be precisely determined from laboratory calibrations. The specific organic components of seawater that produce absorption in the UV and their concentrations are not well

characterized, however. We have approximated the background spectrum due to colored dissolved organic matter (CDOM) by a simple quadratic function of wavelength (Holm et al., 1997; Thomas et al., 1990). Eq. (2) then becomes

$$A_\lambda = b(\Sigma_J \varepsilon_{\lambda,J} C_J + e + f\lambda + g\lambda^2), \quad (3)$$

where the summation runs over inorganic ions only. Concentrations are determined by fitting Eq. (3) to the observed absorbance spectrum in each sample with a linear, least-squares optimization (Press et al., 1986). The C_J concentration values and e, f and g baseline coefficients are all treated as adjustable parameters.

Measurements of the UV absorption spectrum of CDOM in seawater fit an exponential function (Bricaud et al., 1981; Green and Blough, 1994; Guenther et al., 2001). However, we found that the use of an exponential function was problematic for several reasons. First, an exponential baseline function requires a non-linear, least-squares algorithm to solve for the chemical concentrations. A non-linear model uses significantly more computational time for convergence than does a linear algorithm, which can be used to solve Eq. (3). Further, it is possible that non-linear algorithms may diverge if initial estimates of the adjustable parameters are not close to the proper values. Unless initial estimates of chemical concentrations and background spectral parameters are quite good, it may take significantly longer to compute the results with a non-linear algorithm running on a Model 8 data logger than it does to collect and store the spectra. Finally, instrumental drift may produce negative absorbances and positive baseline slopes, which cannot be fitted by an exponential baseline. As we show below, the quadratic baseline function provides adequate fits to spectra observed in seawater. Further observations will be necessary to verify this for more highly colored waters, but the results of Holm et al. (1997) and Thomas et al. (1990) suggest that the quadratic baseline will be adequate in most cases.

The array of molar absorptivity values for sea salt, which is primarily due to bromide (Collos et al., 1999), was determined by measuring the absorption spectrum of a series of low ($<0.1\,\mu M$) nitrate seawater samples that were prepared by diluting a surface sample (salinity ~ 33.5) with deionized (Millipore Milli-Q) water. The molar absorptivity at each wavelength was determined as the slope of a linear regression of absorbance versus salinity of the sample. The array of molar absorptivity values for nitrate and sulfide were determined by measuring the absorbance of a series of chemical standards prepared in the low nutrient seawater. The molar absorptivity was determined from the slope of a linear regression of standard absorbance versus standard concentration. Care must be exercised when storing low nutrient seawater samples, which are intended for standardization, because seawater readily picks up large amounts of dissolved organic carbon from plastic carboys. High DOC concentrations in standards or samples bias the molar absorptivity of sea salt and produce erroneous nitrate and salinity results.

3. Results and discussion

3.1. System performance

The design goal for the ISUS was a spectral stability of ~ 0.001 A with a 1 cm optical path length. This corresponds to an estimated sensitivity for nitrate of

$$\begin{aligned}\Delta NO_3 &= \pm 0.001/4000\,\text{l/mol/cm/1 cm} \\ &\quad \times 10^6\,\text{mmol/mol} \\ &= \pm 0.25\,\text{mM}, \end{aligned} \quad (4)$$

where 4000 l/mol/cm is the approximate molar absorptivity of nitrate at a wavelength of 216 nm (e.g., Fig. 1). The absolute stability did not reach this level, and absorbance would drift up to values of 0.2 after several months. However, these intensity changes were proportional, or nearly so, across the entire spectrum. As a result, the drift corresponds to an offset in absorbance that can be fit with a linear equation. Such an offset is subsumed in the terms $e + f\lambda$ of the spectral model in Eq. (3). The high resolution spectrometer allows these terms of the baseline to be constrained by measurements in the region >250 nm where there is little absorbance due to inorganic ions. The

actual system performance can be assessed, in part, by analyzing the quality of the model fit to spectra. Representative spectra collected in situ with the ISUS system at 5 and 100 m in Monterey Bay are shown in Fig. 3A and B. The spectra were fitted to Eq. (3) over a wavelength range from 215 to 270 nm using the array of molar absorptivities for sea salt and nitrate. The residuals of the fit are shown in Fig. 3E and F. The largest residual values are on the order of 0.001 A for these scans. Typical spectra collected throughout this study yield a root mean square residual value of 0.001–0.002 A in the region where Eq. (3) is fitted. Short-term noise in the system is close to the target specification for the system and the spectral model corrects for long-term drift.

The uniformity of the residuals across the spectrum indicates that the spectral model represented by Eq. (3) contains all of the major signals in the spectra of coastal seawater. Ultraviolet absorption by CDOM in coastal seawater must be adequately represented by the quadratic model. The spectrum of CDOM is often characterized by a maximum in the 260 nm region when it is present at high concentrations (Guenther et al., 2001). The spectra in Fig. 3A and B are plotted on an expanded scale in Figs. 3C and D. There is clearly a significant difference in the baseline slope

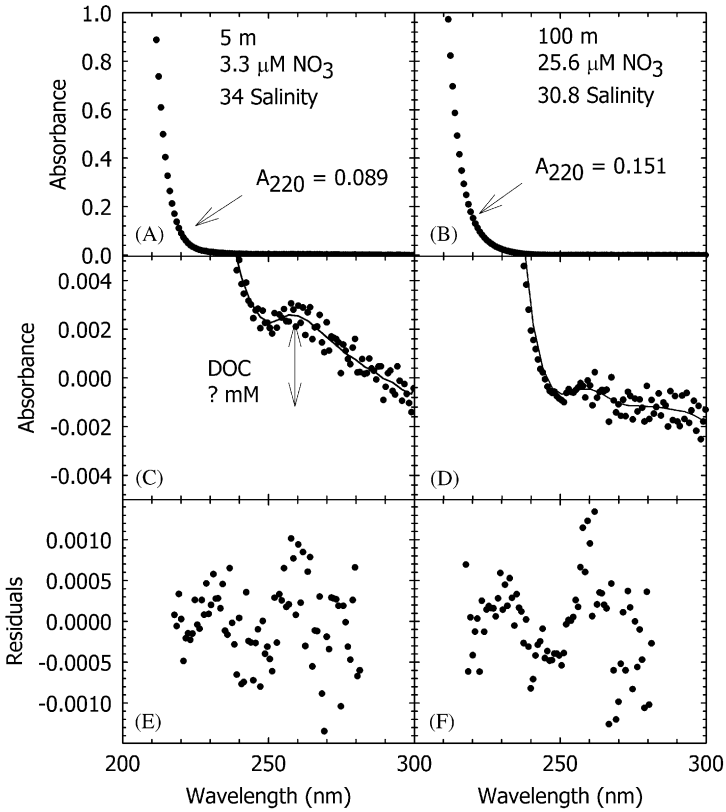

Fig. 3. (A) Spectra measured in situ with ISUS at 5 m. Calculated nitrate concentration is 3.3 μM and salinity is 34. Absorbance at 220 nm is 0.089. (B) Spectra measured in situ with ISUS at 100 m. Calculated nitrate concentration if 25.6 μM and salinity is 30.8. Absorbance at 220 nm is 0.151. (C) Same spectra as in (A), on an expanded absorbance scale. Note the peak at 260 nm and relatively steep baseline slope, which may indicate more dissolved organic carbon than in the 100 m sample. (D) Same spectra as in (B), on an expanded absorbance scale. (E) Residual values from a regression of Eq. (3) to the 5 m spectra over the range 215–270 nm. (F) Residual values from a regression of Eq. (3) to the 100 m spectra. The profile was collected in Monterey Bay on May 22, 2000. Path length was 1 cm.

(245–300 nm) of the spectra collected within the euphotic zone at approximately 5 m (depth was determined from wire out), as compared to a 100 m sample that was well below the thermocline and the euphotic zone. The 5 m spectrum has a much steeper baseline and there is some evidence of a small (<0.001 A) spectral peak near 250 nm. These results suggest that the 5 m sample had more CDOM than did the 100 m sample. However, in both cases, the quadratic baseline function appears to be an adequate fit. We did not try to resolve the spectra of nitrite in any of the work reported here. Nitrite concentrations are generally $<1\,\mu M$ in the region where we have conducted our field tests.

The spectral model incorporated into Eq. (3) does not contain any pressure or temperature correction terms. Environmental parameters may affect the operation of the system by changing molar absorptivities of chemical species (Di Noto and Mecozzi, 1997) or by changing the performance of the spectrometer itself. The effects of temperature and pressure on sensor response were estimated by placing a 25 ml polyethylene bottle containing deionized water, surface seawater with low nitrate concentrations ($<2\,\mu M$), or the surface seawater plus 40 μM nitrate over the sensor head and lowering the instrument to 400 m at 30 m/min. Vertical profiles of chemical concentrations estimated from these tests are shown in Fig. 4, based on the down casts. Small, but significant, changes in the estimated salinity and nitrate concentration of deionized water occur from the surface to depth (Fig. 4A and B). The estimated salinity at depth is approximately 0.4 less than the salinity estimated at the surface when the system is calibrated on the Practical Salinity Scale. Despite this trend, the mean and standard deviation for all of the nitrate measurements in deionized water was $-0.08 \pm 0.28\,\mu M$ (1 SD), while the optical salinity estimate was 0.03 ± 0.13 using seawater standards calibrated on the Practical Salinity Scale ($n = 1100$). The variability of the nitrate measurement is approximately equal to that predicted by Eq. (4).

There is a clear decrease with depth in the salinity estimates derived from spectral scans of the seawater samples (Fig. 4C and E). This decrease in optical salinity from values near 33.5

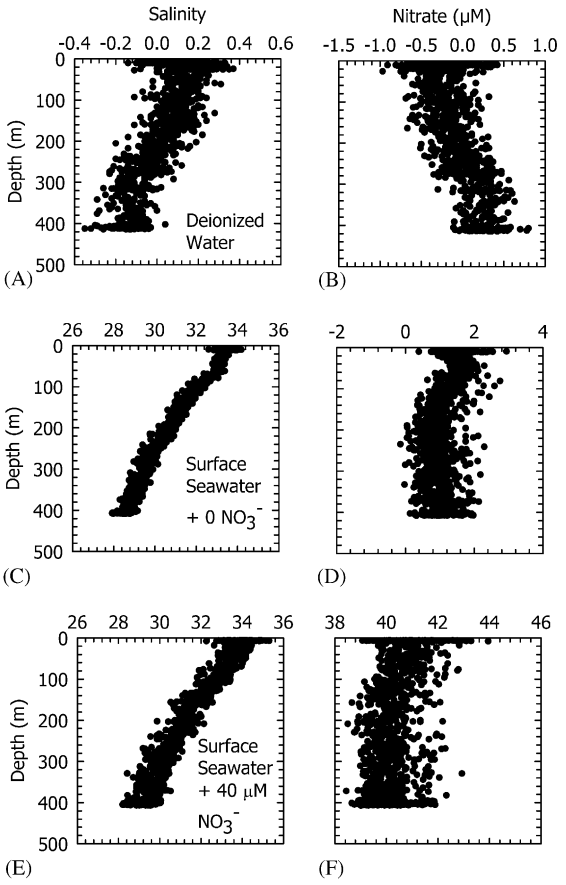

Fig. 4. Vertical profiles to 400 m with calibration solutions on retroreflection probe tip. Only the down casts are shown. (A) Salinity calculated with deionized water solution, (B) nitrate calculated with deionized water solution, (C) salinity calculated from bromide concentration in a surface seawater sample, (D) nitrate calculated in surface seawater sample, (E) salinity calculated in surface seawater sample with 40 μM nitrate added, and (F) nitrate calculated in surface seawater with 40 μM nitrate added.

at the surface to 29 at 400 m contrasts with a salinity increase from 33.5 at the surface to 34.3 at 400 m, which was observed with a CTD on the same casts. The molar absorptivities of seasalt and nitrate show much smaller changes with temperature. The salinity decrease appears to be due to a non-linear increase in the intensity of the lamp at the lowest wavelengths as the ISUS enters colder water. Further tests are required to more fully characterize the effect of temperature on instrument performance.

The mean nitrate concentrations for the entire up and down profiles with both seawater samples are $1.44 \pm 0.66\,\mu M$ ($n = 2300$) and $40.7 \pm 1.0\,\mu M$ ($n = 2100$). The standard deviation for nitrate measurements in low nitrate surface seawater was nearly 3-fold higher than for nitrate measurements in deionized water. The increased error for nitrate measurements in seawater, relative to deionized water, is consistent with a constant noise on the detector array, but decreased signal in seawater due to light absorption by bromide. Constant detector noise creates a much larger change in absorbance signal when the incident light intensity through the sample is attenuated by sea salt. The instrument precision will invariably be better in fresh water than in salt water, therefore.

3.2. Vertical profiling for nitrate

The accuracy of the system was further assessed by mounting ISUS on a CTD/rosette and comparing nitrate concentrations derived from vertical profiles with nitrate measured in bottle samples from the same casts. Profiles were collected over the course of a 2-week research cruise off central California. The discrete samples were collected with a rosette sampler on the up casts, frozen and then analyzed on shore with an Alpkem RFA segmented flow analyzer (Sakamoto et al., 1990). The segmented flow method incorporates the conventional cadmium reduction column to reduce nitrate to nitrite, followed by derivatization of nitrite to form a pink azo dye.

A series of vertical profiles of nitrate to 200 m determined with ISUS and in the laboratory by autoanalyzer are shown in Fig. 5. The ISUS was zeroed five times over the course of the cruise by scanning deionized water ($I_{\lambda,0}$) in order to calculate absorbance from Eq. (1). The optical estimates of nitrate concentration are highly correlated ($R^2 = 0.98$) with the conventional measurements made by the cadmium reduction method. The nitrate concentrations determined in situ by UV spectrophotometry do an excellent job of reproducing the shape of the vertical nitrate profile determined with the bottle samples. However, there appears to be a slight underestimate of the deepest nitrate concentrations measured in bottle

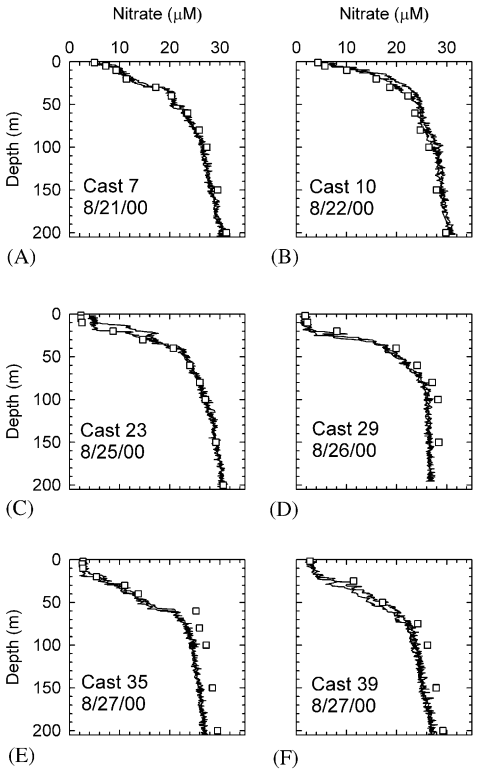

Fig. 5. Vertical nitrate concentration profiles calculated from a series of hydrocasts in Monterey Bay to 200 m depth. Up and down casts are shown. Nitrate concentration profiles determined with an Alpkem RFA autoanalyzer in water samples collected on the up cast are plotted as open squares.

samples, particularly on Casts 29–39 (Fig. 5D–F). This is seen more clearly on Cast 16 to 500 m (Fig. 6). On this profile, the optical nitrate values, which are derived using spectra measured at room temperature in the laboratory for each chemical species ($\varepsilon_{\lambda,J}$), underestimate the observed nitrate concentrations by 13% at 500 m depth (Fig. 6A). A linear regression of the ISUS data versus the RFA nitrate data was $NO_3ISUS = 1.47 + 0.905\,NO_3RFA$ ($n = 70$, $R^2 = 0.979$) for the entire data set. A similar underestimate of the concentration of nitrate ($\sim 10\%$) was observed, when surface seawater plus 40 μM nitrate was contained in a bottle on the retroreflection probe and the instrument was lowered to 400 m (Fig. 4F). Our data imply that the underestimate at depth is

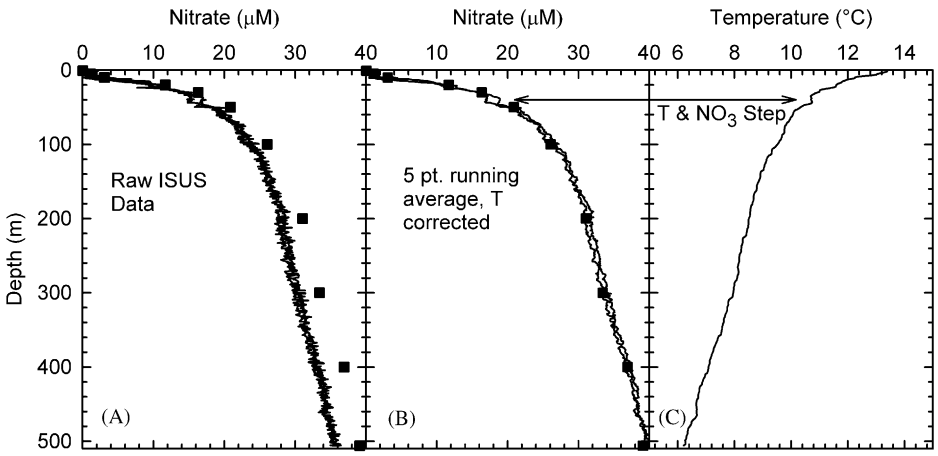

Fig. 6. (A) Vertical nitrate concentration profile to 500 m on up and down cast in Monterey Bay. Nitrate concentration profiles determined with an Alpkem RFA autoanalyzer in water samples collected on the up cast are plotted as open squares. ISUS spectra were collected at 0.6 Hz. (B) As in (A) except ISUS profiles were smoothed by applying a 5 point running mean. Values were then temperature corrected by increasing the nitrate values by the same proportion as the error in optical salinity. (C) Temperature profile on down cast.

primarily temperature related. On Casts 10 and 23, the optical nitrate values are too high by several micromolar near the surface, which biases the zero intercept of the linear regression high. This may reflect an error in the zero scan used for these two profiles that biases all of the nitrate concentrations to high values. Such a high bias at the surface would obscure a depth dependent underestimate as seen on other profiles.

Optical nitrate measurements appear to require a correction for the impacts of temperature on instrument performance. It is clear from our preliminary observations that the temperature correction required for optical nitrate measurements will be considerably smaller than that which is needed for salinity measurements made by electrical conductivity or oxygen measurements with a Clark electrode. It should not be a serious impediment to optical nitrate measurements. The behavior of the optical salinity measurements derived on all of these profiles was similar to the results shown in Fig. 4. In every case, there is reasonable agreement with the salinity value derived from the CTD at the surface. The optical estimates of salinity then decrease to values near 30 at 200 m and reach values of 28 at 500 m. The underestimate of salinity by the UV method is a similar percentage ($\sim$15% at 500 m) as the underestimate of nitrate. One correction scheme would be to increase UV nitrate measurements by the same fraction that the UV salinity underestimates the correct value. When this correction is applied to the data shown here, the UV estimates of nitrate are indistinguishable from the autoanalyzer measurements (Fig. 6B).

The ISUS system is capable of a temporal resolution on the order of 1 s. The sampling rate is limited by the amount of time required to integrate enough light onto the detector array to produce the desired signal to noise ratio. Integration times of 1 s produce detector signal on the order of 10,000 counts at 216 nm in deionized water. A typical peak to peak electronic noise in the detector of approximately 50 counts corresponds to an absorbance noise of $\sim$0.002 A for a 10,000 count signal. This is near the maximum acceptable. Shorter integration times would produce nitrate concentrations with lower precision using the current system. This may be partially compensated for by averaging greater numbers of scans. However, the detector dark current becomes a much greater factor at low light intensities and

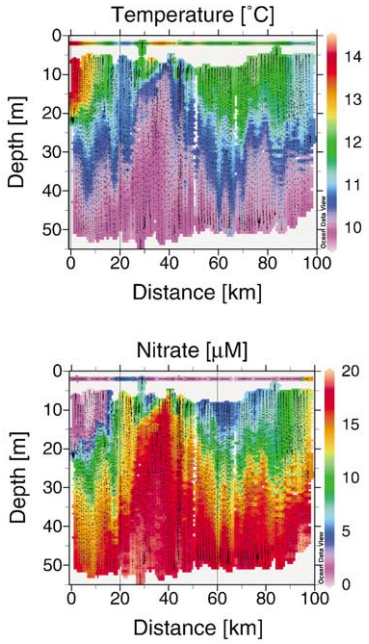

Fig. 7. (A) Temperature and (B) nitrate determined with ISUS and an FSI MicroCTD mounted on a SeaSciences Acrobat undulating vehicle. Nitrate and temperature data were binned to 3 s averages and each point is shown as a black dot. The acrobat was towed in a U-shaped pattern from warm offshore waters through an upwelling source area along the coast north of Santa Cruz, CA near 40 km along the tow, and then back offshore at 70 km and then back towards the upwelling source area. There are some 70 complete vertical cycles along the 100 km path. The nitrate data at 2 m depth were determined with an Alpkem RFA autoanalyzer interfaced to the ships scientific water supply. The 2 m temperature data are from a thermosalinograph in the same seawater system. Tow speed was approximately 10 km/h.

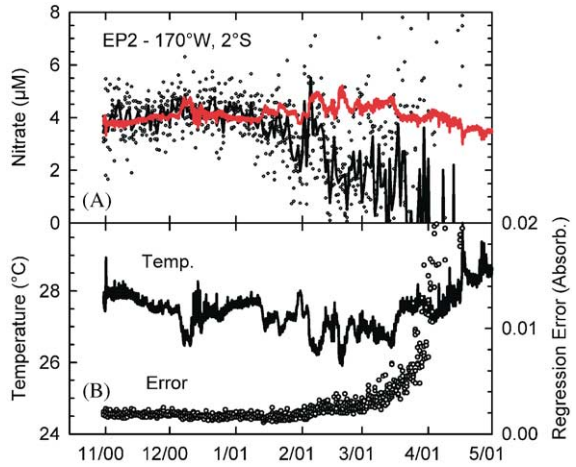

Fig. 8. (A) Nitrate concentrations measured at 2 m depth from the EP2 mooring in the TAO/TRITON array at 2°S, 170°W. Five measurements were made each day within a 10 s span. The solid black line shows the daily average and the individual concentrations from each scan are shown as circles. The red line shows nitrate concentrations predicted from a quadratic equation in temperature fitted to observations in this region (Chavez et al., 1996). Temperature from a CT sensor on the mooring was used to predict nitrate. (B) Temperature from CT sensor on the mooring (—) and the standard deviation of the regression (absorbance units) for each spectral scan (○).

systematic errors due to the dark current correction can be large.

The ISUS is capable of resolving nitrate variability on a scale of 50 cm at a vertical profiling speed of 30 m/min and a sampling rate of 1/s, assuming that the approximately 1 cm^3 sample volume of the retroreflection probe is completely flushed between each sample. This assumption seems entirely reasonable, given the small volume and exposed position of the probe. At lower profiling speeds, the limit on spatial resolution is the 0.5 cm length of the illuminated region of the retroreflection probe.

The raw nitrate data for a vertical profile to 500 m is shown in Fig. 6A. The calculated nitrate concentrations have a standard deviation on the order of 0.6 µM when the instrument is held at a constant depth near the surface. This is similar to the variability observed in Fig. 4D and F. Further, the up and down casts for the vertical profiles shown in both Figs. 7 and 8 are quite similar. This indicates that there is negligible drift in the instrument over the time period of a cast. Signal averaging can, therefore, produce a significant improvement in detection limits, as shown by the difference between Fig. 6A and B. A 5 point moving average, which corresponds to 2–3 m depth bins, produces a considerably smoother profile (Fig. 6B). The smoothed profile still resolves many of the small scale features seen in the temperature profile, including a distinct temperature and nitrate step near 40 m depth (Fig. 6C).

The conventional detection limit, expressed as 3 SD, is 1.8 µM. However, if the detection limit is

expressed as the 95% confidence interval, it can be made quite low by simply averaging a number of observations. For example, the 95% confidence interval = $2.04\,SD/30^{0.5} = 0.2\,\mu M$ for a 30 s average. The practical detection limit is somewhat higher, as evidenced by the offsets high and low at the surface for the various casts shown in Fig. 5. These offsets seem to be introduced by small errors in the various deionized water calibration spectra that result from tiny air bubbles trapped in the retroreflection probe. We are now calibrating the system with a slight over pressure on the deionized water solution to eliminate these bubbles.

3.3. Performance on towed, undulating vehicle

Long-term stability of the optical components is key to routine operation of the instrument. The results shown in Fig. 5 demonstrate the stability of the instrument when used intermittently (37 total casts) over a 2-week period. There are no large systematic changes in time. If a single zero scan is used for the entire period, agreement between the UV and RFA methods is only slightly degraded ($R^2 = 0.95$). A second instrument was operated on a Sea Sciences Acrobat undulating vehicle for several tows of up to 12 h duration on the same cruise. The ISUS was operated continuously during these tows with no opportunity for recalibration. Fig. 7 shows the variability in nitrate and temperature observed over one tow of 11 h duration. A segmented, continuous flow analyzer was operated on board the ship to analyze water from the scientific seawater supply, which originates at 2 m depth, during the same tow. At the termination of the tow, the ISUS reported nitrate concentrations of 12.7 μM as it was brought through 2 m for recovery. The ship board analyzer reported concentrations of 14.7 μM at the same time. The optical nitrate value is slightly lower than detected by conventional colorimetric chemistry, which is consistent with all of our other observations in cold seawater (Fig. 5).

3.4. Mooring deployment

The stability demonstrated in Fig. 7 suggests that ISUS is capable of long-term operation on oceanographic moorings. A 6-month record collected with a system deployed at 2 m on the EP2 mooring of the TAO/TRITON array at 2°S, 170°W in the equatorial Pacific is shown in Fig. 8. The retroreflection probe was protected from biofouling with a copper housing that fit snugly over the probe and which had 6 cm long, 0.5 cm inside diameter copper tubes on the inlet and outlet sides. Flushing of the system was passive. Copper shutters have been proposed as a control for biofouling on optical instruments (Chavez et al., 2000). However, copper also absorbs light strongly in the UV region and this may bias the spectra if sufficient flushing does not occur.

Fouling of the system, the presence of UV-absorbing chemical species (including copper) that do not fit the spectral model in Eq. (3), or large, spectral changes in the lamp output can be detected by examining the standard error of the regression (root mean square of the residual absorbance values). Typical values of the standard error of the regression are <0.002 A for systems operated in the laboratory and for short-term deployments in the ocean (Fig. 3E and F). The spectra collected with ISUS deployed on EP2 produced regression standard errors that were nearly constant and <0.002 A for 3 months (Fig. 8C). The nitrate concentrations calculated during this period are generally within the range of 2–4 μM (Fig. 8A), which is consistent with many previous observations near this mooring (e.g., Chavez and Brusca, 1991; Lefevre et al., 1994). Prediction of the nitrate concentrations using the nitrate–temperature relationship defined by Chavez et al. (1996) gives excellent agreement with the daily average value observed with ISUS. The ISUS was operated in a burst mode during this period with five measurements made during a single 10 s period each day. The average value of the standard deviation for each set of five measurements made during the first 3 months of the deployment was 0.7 μM, which is consistent with the nitrate variability seen on vertical profiles (Fig. 4D and 6A). All these results indicate no degradation in performance, relative to that achieved in the laboratory, over a 3-month period on an open ocean mooring. The standard error of the

regression increased slightly during the fourth month (Fig. 8C), although the nitrate concentrations generally remain consistent with expectations. After the fourth month, the standard error of the regression increased rapidly (Fig. 8C) and nitrate concentrations become inconsistent, including many negative values.

The standard error of the regression is a quantitative diagnostic of instrument performance. It clearly demonstrates fouling of the retroreflection probe after the fourth month of operation and perhaps beginning after the third month. The fouling appeared to have been due to copper minerals precipitating on the optical surfaces of the retroreflection probe, rather than biofouling. A second ISUS deployed on mooring EP1, which had longer (12 cm) copper tubes protecting the retroreflection probe, fouled much more quickly (<1 month) than did the EP2 instrument.

3.5. Bisulfide measurements in the benthic boundary layer

Bisulfide ion (HS^-) also absorbs in the ultraviolet with a peak near 230 nm (Fig. 1; Guenther et al., 2001). The ISUS has been used to measure sulfide concentration over cold seeps in the Monterey Bay (Barry et al., 1996; Orange et al., 1999) at depths of 960 m. ISUS deployments were made using the remotely operated vehicle VENTANA. Copper anti-fouling protection was not used on these deployments to avoid chemical reactions with sulfide.

The UV spectrum observed in the benthic boundary layer over a cold seep has a strong spectral component that is very similar to HS^- (Fig. 9). Reconstruction of the observed spectra with salinity, nitrate, sulfide and a constant baseline component reproduces all of the major features observed in the spectra from the boundary layer (Fig. 9). The UV spectra indicate that HS^- is present at concentrations up to 400 μM (all data not shown). Water samples collected within the boundary layer and analyzed by the methylene blue method (Cline, 1969) confirm the presence of hydrogen sulfide at levels similar to those detected with the ISUS, although exact comparisons are difficult due to large spatial and temporal variability within the boundary layer. The HS^- concentrations determined with ISUS decay away from the sediment–water interface rapidly, as would be expected for a chemical species with a benthic source (Fig. 10). The HS^- signal is also not

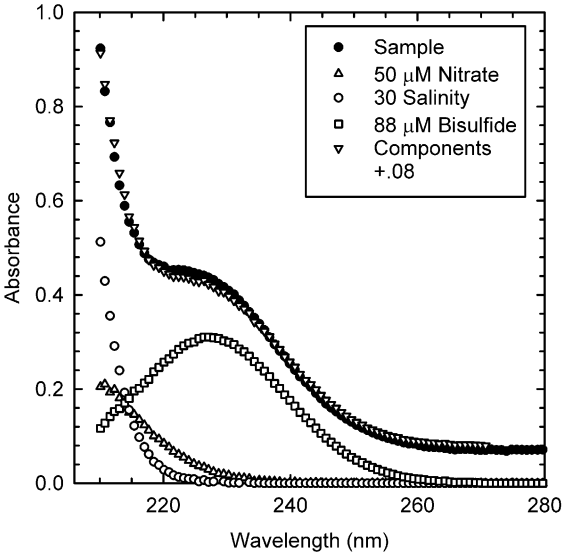

Fig. 9. UV spectra (●) collected in situ at 970 m depth and 1 cm above the bottom over the Extrovert Cliff cold seep (36°46′ 31N long:122°51′ 12W). The modeled component spectra for bisulfide, nitrate and salinity are also shown along with an approximate reconstruction of the observed spectra using a constant (0.08 A) baseline, rather than a quadratic function.

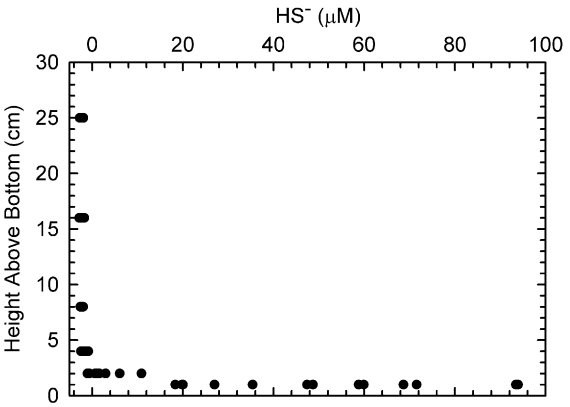

Fig. 10. A vertical profile of bisulfide concentration at the Extrovert Cliff cold seep site. Spectra were collected once in every 5 s.

seen within the boundary layer at sites away from the cold seeps. The background concentration calculated from the spectra recorded well away from the bottom is -2.5 ± 0.4 (1 SD; $n = 250$) μM HS^-. The slightly negative value may again reflect greater lamp output at low temperature. These results demonstrate the ability of the ISUS to collect measurements with a spatial resolution on the order of 1 cm.

4. Conclusion

High resolution, ultraviolet spectrophotometry now appears to be a feasible method for the direct measurement of nitrate and bisulfide ion in situ. The spectral model that we describe compensates for the largest components of instrumental drift, which makes it possible to use in situ spectrophotometers for long periods of time without recalibration. The remaining artifacts due to temperature effects on instrumental performance can be corrected by normalizing estimated concentrations by the error in the optical estimate of salinity. Systematic errors due to non-linear instrumental drift or additional UV-absorbing chemical species that are not included in the spectral model can be readily identified due to a large increase in the residuals of the spectral model (Guenther et al., 2001). The most important exception to the current capabilities of ISUS would be the very low nitrate concentrations (< 300 nM) found in the surface waters of the oligotrophic open ocean. However, it may be feasible to use much longer path length cells, including liquid core waveguides, to achieve large reductions in the detection limit (Belz et al., 1998).

Acknowledgements

This work was supported by NSF Grant OCE 9906983 and by a grant from the David and Lucile Packard Foundation. Thanks to Steve Fitzwater, Carole Sakamoto, Ginger Elrod, Peter Walz, Francisco Chavez, Gene Massion, Jon Erickson, Jim Scholfield and Dick Littlefield for their assistance on this project and to the crews of the Research Vessels NEW HORIZON, POINT LOBOS and JOHN H. MARTIN.

References

Armstrong, F.A.J., Boalch, G.T., 1961. The ultra-violet absorption of seawater. Journal of the Marine Biological Association, UK 41, 591–597.

Barry, J.P., Greene, H.G., Orange, D.L., Baxter, C.H., Robison, B.H., Kochevar, R.E., Nybakken, J.W., Reed, D.L., Mchugh, C.M., 1996. Biologic and geologic characteristics of cold seeps in Monterey Bay, California. Deep-Sea Research I 43, 1739–1762.

Bastin, R., Weberling, T., Palilla, F., 1957. Ultraviolet spectrophotometric determination of nitrate. Analytical Chemistry 29, 1795–1797.

Belz, M., Press, P., Klein, K.-F., Boyle, W.J.O., Franke, H., Grattan, K.T.V., 1998. Liquid core waveguide with fiber optic coupling for remote pollution monitoring in the deep ultraviolet. Water Science Technology 37, 279–284.

Berger, A.J., Koo, T.-W., Itzkan, I., Feld, M.S., 1998. An enhanced algorithm for linear multivariate calibration. Analytical Chemistry 70, 623–627.

Bricaud, A., Morel, A., Prieur, L., 1981. Absorption by dissolved organic matter of the sea (yellow substance) in the UV and visible domains. Limnology and Oceanography 26, 43–53.

Buck, R.P., Singhadeja, S., Rogers, L.B., 1954. Ultraviolet absorption spectra of some inorganic ions in aqueous solutions. Analytical Chemistry 26, 1240–1242.

Buffle, J., Horvai, G. (Eds.), 2000. In Situ Monitoring of Aquatic Systems: Chemical Analysis and Speciation. Wiley, New York.

Chavez, F.P., Brusca, R.C., 1991. The Galapagos Islands and their relation to oceanographic processes in the tropical Pacific. In: James, M.J. (Ed.), Galapagos Marine Invertebrates. Plenum Press, New York, pp. 9–33.

Chavez, F.P., Service, S.K., Buttrey, S.E., 1996. Temperature–nitrate relationships in the central and eastern tropical Pacific. Journal of Geophysical Research 101, 20553–20563.

Chavez, F.P., Wright, D., Herlien, R., Kelley, M., Shane, F., Strutton, P.G., 2000. A device for protecting moored spectroradiometers from bio-fouling. Journal of Oceanographic and Atmospheric Technology 17, 215–219.

Clayson, C.H., 2000. Sensing of nitrate concentration by UV absorption spectrophotometry. In: Varney, M. (Ed.), Chemical Sensors in Oceanography. Gordon and Breach, London, pp. 107–121.

Clesceri, L.S., Greenberg, A.E., Trussell, R.R. (Eds.), 1989. Standard Methods for the Examination of Water and Wastewater, 17th Edition. American Public Health Association, Washington, DC, pp. 4-132–4-133.

Cline, J.R., 1969. Spectrophotometric determination of hydrogen sulfide in natural waters. Limnology and Oceanography 14, 454–458.

Collos, Y., Mornet, F., Sciandra, A., Waser, N., Larson, A., Harrison, P.J., 1999. An optical method for the rapid measurement of micromolar concentrations of nitrate in marine phytoplankton cultures. Journal of Applied Phycology 11, 179–184.

Di Noto, V., Mecozzi, M., 1997. Determination of seawater salinity by ultraviolet spectroscopic measurements. Applied Spectroscopy 51, 1294–1302.

Dickey, T., Marra, J., Granata, T., Langdon, C., Hamilton, M., Wiggert, J., Siegel, D., Bratkovich, A., 1991. Concurrent high resolution bio-optical and physical time series observations in the Sargasso Sea during the spring of 1987. Journal of Geophysical Research 96, 8643–8663.

Finch, M.S., Hydes, D.J., Clayson, C.H., Weigl, B., Dakin, J., Gwillam, P., 1998. A low power ultra violet spectrophotometer for measurement of nitrate in seawater: introduction, calibration and initial sea trials. Analytica Chimica Acta 377, 167–177.

Green, S.A., Blough, N.V., 1994. Optical absorption and fluorescence properties of chromophoric dissolved organic matter in natural waters. Limnology and Oceanography 39, 1903–1916.

Guenther, E.A., Johnson, K.S., Coale, K.H., 2001. Direct ultraviolet spectrophotometric determination of total sulfide and iodide in natural waters. Analytical Chemistry 73, 3481–3487.

Holm, T.R., Kelley, W.H., Sievers, L.F., Webb, D.L., 1997. A comparison of ultraviolet spectroscopy with other methods for the determination of nitrate in water. Spectroscopy 12, 38–45.

Huebner, M., Meyer, H., Klein, K.-F., Hillrichs, G., Retting, M., Veidemanis, M., Spangenberg, B., Clarkin, J., Nelson, G., 2000. Fiber-optic systems in the uv-region. In: Vo-Dinh, T., Grundfest, W.S., Benaron, D.A. (Eds.), Proceedings of the SPIE, Vol. 3911, Biomedical Diagnostic, Guidance, and Surgical-Assist Systems II. SPIE Press, Bellingham, WA, pp. 303–312.

Johnson, K.S., Jannasch, H.W., 1994. Analytical chemistry under the sea surface: monitoring ocean chemistry in situ. Naval Research Reviews XLVI (3), 4–12.

Johnson, K.S., Beehler, C.L., Sakamoto-Arnold, C.M., Childress, J.J., 1986. In situ measurements of chemical distributions in a deep-sea hydrothermal vent field. Science 231, 1139–1141.

Karlsson, M., Karlberg, B., Olsson, R.J.O., 1995. Determination of nitrate in municipal waste water by UV spectroscopy. Analytica Chimica Acta 312, 107–113.

Lefevre, N., Andrie, C., Dandonneau, Y., Reverdin, G., Rodier, M., 1994. PCO_2, chemical properties, and estimated new production in the equatorial Pacific in January–March 1991. Journal of Geophysical Research 99, 12639–12654.

McGillicuddy Jr., D.J., Robinson, A.R., Siegel, D.A., Jannasch, H.W., Johnson, R., Dickey, T.D., McNeil, J., Michaels, A.F., Knapp A, .H., 1998. Influence of mesoscale eddies on new production in the Sargasso Sea. Nature 394, 263–266.

Menzel, R., Juilfs, G., Schroeder, F., Knauth, H.-D., 1997. Applicability and limits of a new in situ nitrate analyzer. Special emphasis to seawater analysis. In: Proceedings of the March'h Mor Workshop. IUEM Brest, France, pp. 193–201.

National Research Council, 2000. Illuminating the Hidden Planet: The Future of Seafloor Observatory Science. National Academy Press, Washington, DC.

Ogura, N., Hanya, T., 1966. Nature of ultra-violet absorption in sea water. Nature 212, 758.

Orange, D.L., Greene, H.G., Reed, D., Martin, J.B., McHugh, C.M., Ryan, W.B.F., Maher, N.M., Stakes, D.S., Barry, J.P., 1999. Widespread fluid expulsion on a translational continental margin: mud volcanoes, fault zones, headless canyons, and aquifers in Monterey Bay, California. Geological Society of America, Bulletin 111, 992–751009.

Press, W.H., Flannery, B.P., Teukolsky, S.A., Vetterling, W.T., 1986. Numerical Recipes, The Art of Scientific Computing. Cambridge University Press, Cambridge.

Rutan, S.C., 1991. Adaptive Kalman filtering. Analytical Chemistry 63, 1103A–1109A.

Sakamoto, S.M., Friederich, G.E., Codispoti, L.A., 1990. MBARI procedures for automated nutrient analyses using a modified Alpkem Series 300 Rapid Flow Analyzer. Technical Report No. 90-2, Monterey Bay Aquarium Research Institute.

Smith, J.P., 2000. Spectrometers get small. Analytical Chemistry 72, 653A–658A.

Thomas, O., Gallot, S., 1990. Ultraviolet multiwavelength absorptiometry (UVMA) for the examination of natural waters and waste waters: Part I: general considerations. Fresenius Journal of Analytical Chemistry 338, 234–237.

Thomas, O., Gallot, S., Mazas, N., 1990. Ultraviolet multiwavelength absorptiometry (UVMA) for the examination of natural waters and waste waters: Part II: determination of nitrate. Fresenius Journal of Analytical Chemistry 338, 238–240.

Varney, M.S. (Ed.), 2000. Chemical Sensors in Oceanography. Gordon and Breach, New York.